

Outer Concrete Containments of LNG-Tanks – Design against Thermal Shock

Josef Roetzer

Dywidag International, Munich, Germany

Theodor Baumann

Munich, Germany

ABSTRACT: The stability and tightness of the concrete outer tank has to be guaranteed by an appropriate design also under cryogenic conditions. The relevant codes provide a lot of formal regulations, but give no precise indications for analytical procedures and criteria which have to be applied in the design. Hence, the following paper deals with the behaviour of reinforced and prestressed concrete sections in direct contact with LNG, considering thermal strains and consecutive crack formation. Mechanical models, which have to be clear and simple, are discussed. The course of sectional forces and displacements due to a temperature gradient of 180°C after failure of the inner tank are outlined for areas below and above the LNG level. Substantial design criteria are proposed and discussed. Essential in this respect are the thickness of the residual compressive zone, the reinforcement steel stresses and the characteristic crack width. By means of ingenious models, a way for the direct understanding of the coherence between the strains and deformations imposed by the temperature gradient and the above design criteria is pointed out.

1 FUNCTION OF LNG-TANKS

The storage of liquefied natural gas (LNG) at -165°C is an economic significant and technical demanding task. The concrete outer tank protects the sensitive inner steel tank against external hazards and serves as catch basin in case of failure of the inner tank. This paper deals with the behaviour of the concrete outer tank under the extreme temperature loading caused by the direct contact with LNG.

The application of LNG-technology is based on the physical behaviour of LNG. By cooling down to -165°C the gas is liquefied with a consecutive reduction in volume of 1/600. Thereby the transportation with ships and the appertaining storage in tanks become economically feasible. A state-of-the-art design requires a prestressed concrete outer tank which is able to operate as a catch basin in case of liquid spill. This conception requires even in the emergency case a closed container, which is able to prevent the uncontrolled escape of gas clouds into the environment.

Containments according to this design philosophy are called full containment tanks. They consist of a concrete outer tank and a steel inner tank. The concrete outer tank is composed of a bottom slab, a prestressed wall shell, often with a ring beam on top of the wall, and a reinforced concrete roof. The hydrostatic LNG pressure requires prestressing of the wall in hoop (horizontal) direction. The size of the

vertical prestressing depends primarily on the internal gas overpressure. The liquid gas is stored in the steel inner tank. Adequate ductility of steel at -165°C requires a minimum nickel content of 9%. The inner steel tank is open on top. The LNG is pumped into and out of the tank by cryogenic pumps suspended on the concrete roof.

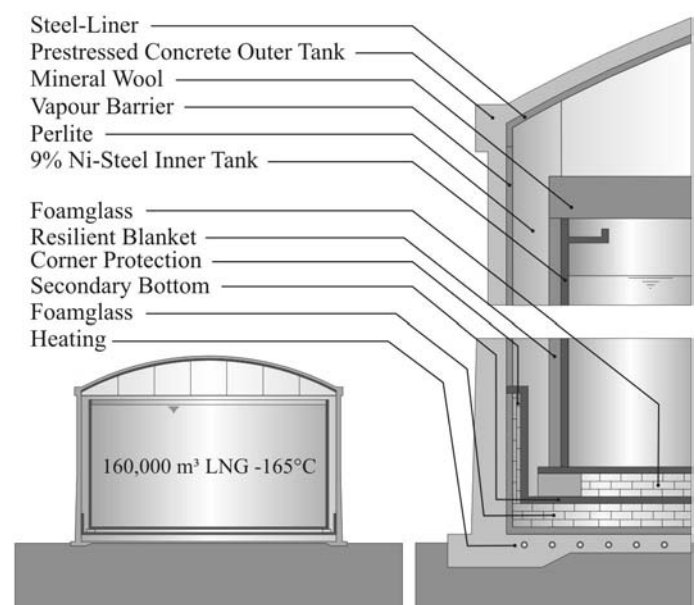


Figure 1: Typical components of a LNG tank

Heat supply is limited by an all side insulation to reduce the evaporation rate of the LNG, which is at -165°C close to the boiling point. Hence, between

concrete outer tank and steel inner tank, a thermal insulation layer of about 1m is necessary.

For layout and design of the concrete outer tank an appropriate assessment of the effect of extreme temperatures is essential. The design criteria are impermeability and stability. Even some through-cracks indicate no catastrophic scenario, as long as the crack width is limited. LNG which is infiltrating into the cracks passes inside the wall into the gaseous state and reaches the wall outer surface not as fluid. The design of the reinforced concrete structure requires the consideration of the nonlinear material behaviour and crack formation. Thereby the sectional forces due to constraint are reduced to a fraction of the values of the uncracked state. The structural analysis shall demonstrate that the cracked wall section is able to bear the pressure from leakage and internal gas overpressure. The common approach of separate assessments for load and for restraint of thermal deformation makes no sense. The analysis of strains is only possible for the common action of loads and imposed deformations.

For design of the reinforced and prestressed concrete walls the liquid spill is the dominant load case, which is furthermore highly complex. For the accuracy to be reached, the understanding of the behaviour of the cracked structure is the most important item. Therefore this paper deals with the relation between the temperature gradient and the resulting stresses, strains and crack widths. Substantial design criteria, which are able to ensure the impermeability of the concrete wall, are discussed and proposed.

2 CODES AND THERMAL PROCESS CONDITIONS

The relevant codes e.g. BS 7777 or EN 14620 provide a lot of formal regulations but give no precise indications for analytical procedures and criteria to be applied in the design. The common way of an detailed FEM-calculation with highly sophisticated algorithms and nonlinear material behaviour makes no sense, if the physical background is not understood by the user.

BS 7777 requires in case of liquid spill the verification of an average concrete stress of 1 N/mm^2 in the residual compressive zone and that the compressive zone is large enough to ensure impermeability. Other codes additionally define the minimum compressive zone to 80mm respectively 100mm and 10% of the cross section height.

For a better understanding of the load case liquid spill, the time dependent events, leakage and cool down of the concrete wall are examined separately. The inner tank has an usable volume of $160,000\text{m}^3$ and the usable volume on the perlite wall insulation is about 4000m^3 . If the leakage is small and the dis-

charge amounts some liters per second, it takes a couple of days until a balanced level is reached.

The cooling down process of the entire wall section is finished, when the temperature gradient within the wall is nearly linear (steady state). For an 80cm concrete wall this process takes about three days (Roetzer et al. 2006). Following this final stage is examined.

3 PROOF OF THE TANK WALL AGAINST DIRECT EFFECT OF LNG

3.1 General

In case of failure of the inner tank, LNG runs into the space filled with perlite between inner and outer tank and gets in direct in contact with the concrete wall. The inner concrete surface suddenly cools down from $+35^\circ\text{C}$ to -165°C . From this results an effective steady state temperature gradient ΔT_L of 180K. Concrete and reinforcement at the layer want to shorten with $\Delta \varepsilon_{TL} = \alpha_T \cdot \Delta T_L$, but the warmer inner wall areas prevent this. Hence, narrow distributed cracks at the concrete surface are generated. The reinforcement stress reaches values in the range of ($\sigma_s = E_s \cdot \alpha_T \cdot \Delta T_L \approx 200,000 \cdot 10^{-5} \cdot 180 \approx 360\text{MPa}$). The subsequent cooling of the wall reduces the reinforcement stress but increases the crack depth. The steady state temperature gradient represents the most unfavorable design case for stability and impermeability of the catch basin. Temperature caused deformations and stresses are much larger than those generated from hydrostatic pressure. For design and analysis it is essential to take the crack formation into account.

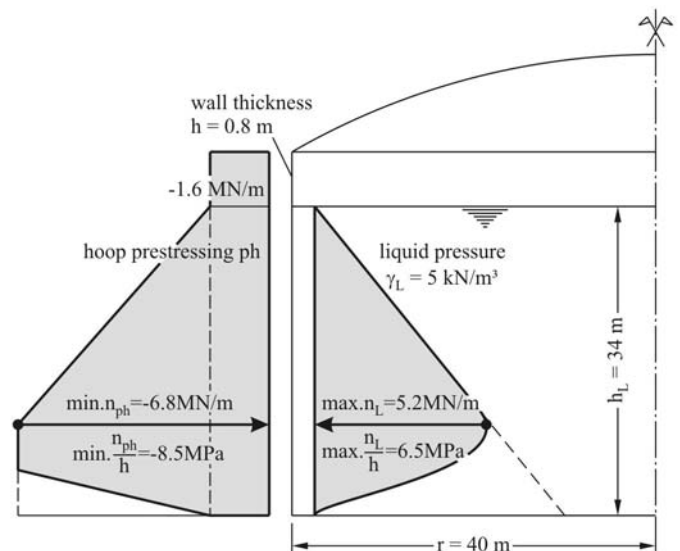


Figure 2: Typical dimensions and hoop forces of a LNG tank

The practical effects are demonstrated for a $160,000\text{m}^3$ tank with a wall thickness of 0.80m. The hoop prestressing has to be set higher than the forces resulting from LNG filling. The residual compress-

sion stress is taken in this example to $(n_L+n_{ph})/h = 6.5 - 8.5 = -2.0\text{MPa}$, see Figure 2.

Figure 3a shows a top view of a wall section without any restraint of deformation (length $2 \cdot l$). The temperature gradient ΔT_L and the related expansion gradient $\Delta \varepsilon_{TL} = \alpha_T \cdot \Delta T_L$ are generating a shortening $\Delta l = 0.5 \cdot \Delta \varepsilon_{TL} \cdot l$ and a corresponding rotation of $\Delta \varphi = \Delta \varepsilon_{TL} \cdot l/h$ at the end of the section. Actually the sections of a cylinder shell are able to shorten, but are not able to distort.

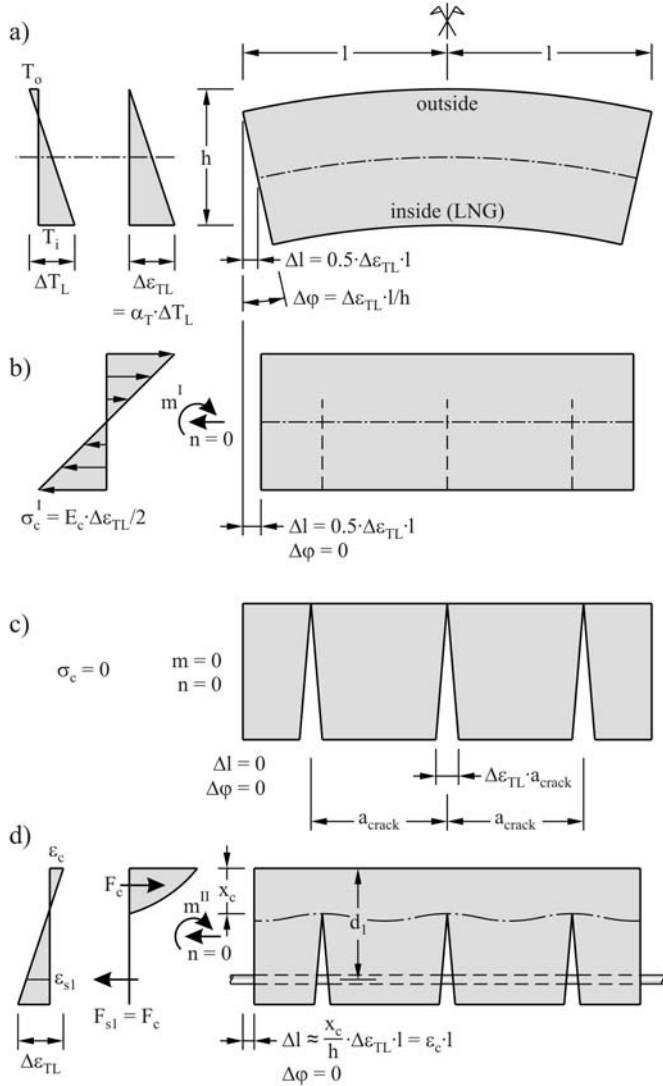


Figure 3: Deformation and cracking of a concrete wall due to direct contact with LNG

Therefore, in hoop direction as well as in meridian direction a restraint moment m^I is generated (see Fig. 3b). Distinct cracks are generated, as the appertaining tensile force σ_c^I is multiple to the tensile strength of concrete. Through-cracks appear if no or only slight reinforcement is placed (Fig. 3c). In case of higher reinforcement content, a restraint moment m^{II} according Figure 3d is generated. The shortening of the neutral axis is calculated with $\Delta l = x_c/h \cdot \Delta \varepsilon_{TL} \cdot l = \varepsilon_c \cdot l$.

The dependence of the strain conditions which are appertaining to the restraint of $\Delta \varepsilon_{TL}$ from the relevant parameters are investigated in section 3.2. The longitudinal force n results either from liquid pressure, internal gas overpressure and horizontal

prestressing in hoop direction or from dead load, internal gas overpressure and vertical prestressing in meridian direction. In the idealisations of Figure 3, $n = 0$ has been assumed. In the real design, a residual compressive force $n < 0$ should be verified.

Temperature related constraint forces are generated not only due to restraint of the gradient $\Delta \varepsilon_{TL}$, but also due to restraint of center line shortening ($\varepsilon_{TL}^{II} = \varepsilon_c$). The required continuous deformation transition from cylinder wall to the not cooled down bottom slab generates in the lower wall region additional bending moments (edge disturbances), whose appearance is explained in Figure 7. This topic is handled in the section 3.3.

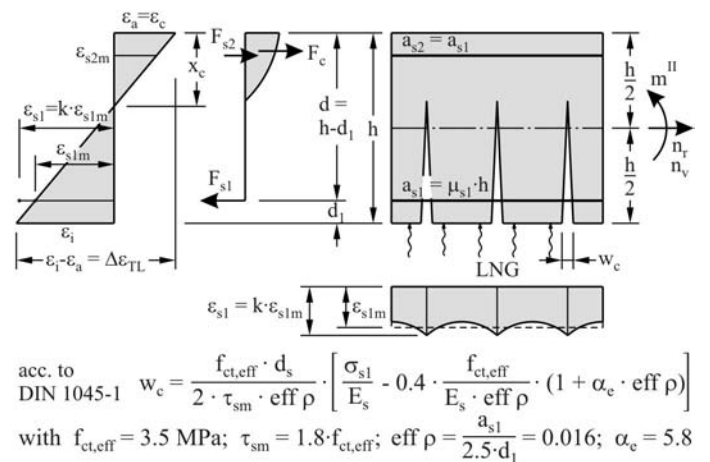
3.2 Restraint of the imposed curvature $\Delta \varepsilon_{TL}/h$

The thermal shortening of the inner side in direct contact with LNG is assumed to $\Delta \varepsilon_{TL} = \alpha_T \cdot \Delta T_L \approx 1.8\text{‰}$. For the superposition of the consecutive curvature $\Delta \varepsilon_{TL}/h$ with the liquid pressure (load case liquid spill) the following values are required:

- x_c thickness of the residual compressive zone
- σ_{s1} inner reinforcement steel stress at the crack
- w_c characteristic crack width at inner wall face

They can be obtained directly with the relations summarized in Figure 4. The detour of a calculation of sectional forces from loading and restraint regarding cracked cross sections with a subsequent dimensioning is not required. The direct approach allows a better understanding of the mechanical significance of the assumptions to be defined.

As a result of the distinct cracking, the tension stiffening effect is low. The ratio $k = \varepsilon_{s1}/\varepsilon_{s1m}$ (maximum to average steel stress) is set to 1.20. The crack widths can be calculated acc. to DIN 1045-1 or acc. to the more consistent continuous crack theory of Noakowski (Noakowski & Schäfer 2003).



$$\text{acc. to DIN 1045-1 } w_c = \frac{f_{ct,eff} \cdot d_s}{2 \cdot \tau_{sm} \cdot \text{eff } \rho} \left[\frac{\sigma_{s1}}{E_s} - 0.4 \cdot \frac{f_{ct,eff}}{E_s \cdot \text{eff } \rho} \cdot (1 + \alpha_e \cdot \text{eff } \rho) \right]$$

with $f_{ct,eff} = 3.5 \text{ MPa}$; $\tau_{sm} = 1.8 \cdot f_{ct,eff}$; $\text{eff } \rho = \frac{a_{s1}}{2.5 \cdot d_1} = 0.016$; $\alpha_e = 5.8$

Figure 4: Sectional strains and forces for LNG-spill

The prestressing forces n_{ph} in horizontal (hoop) and n_{pv} in vertical direction, respectively, are included in the total normal force n_h and n_v . The prestressing tendons are placed in the outer third of

the wall, i.e. near to the neutral axis of the cracked cross section. Therefore the influence of concrete cracking on the tendon forces can be neglected. The eccentricity of the prestressing tendons generates no bending moments, because the shape of the cylinder shell prevents the appertaining curvature.

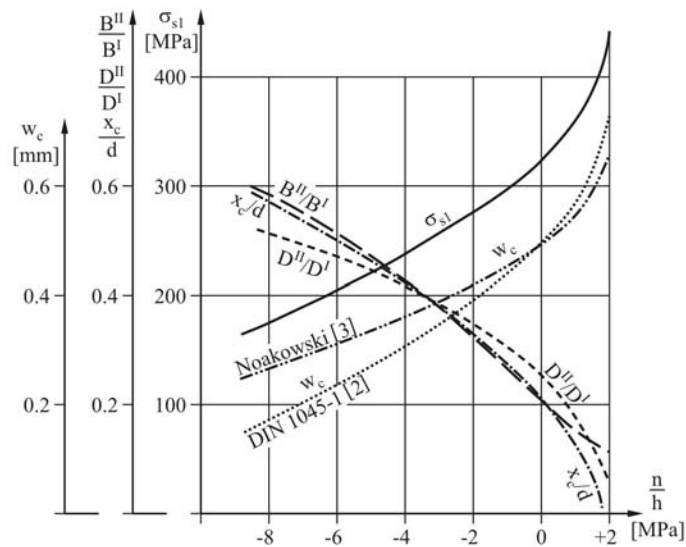


Figure 5: Steel stress, residual compressive zone, crack width and stiffness in dependency from the ratio n/h

Figure 5 and 6 apply to the tank shown in Figure 2. The wall thickness is set to 0.80 m and the reinforcement to $d_s = 25\text{mm}/150\text{mm}$. This corresponds with a reinforcement ratio of $\mu_{s1} = \mu_{s2} = 0.4\%$. The dependency from n/h demonstrates the effect of the prestressing level on the governing criteria of cryogenic design. According to Figure 5 and table 1, the characteristic crack width does not exceed a value of 0.50mm even for a reduction of the residual compressive force (n_h or n_v) to zero.

Table 1: Effect of the residual compressive stress

$(n_L + n_{ph}) / h$	-8 MPa	-2 MPa	0 MPa
x_c	412 mm	234 mm	148 mm
σ_{s1}	175 MPa	276 MPa	324 MPa
w_c	[2] 0.17 mm	0.39 mm	0.49 mm
(for $d_s = 25\text{ mm}$)	[3] 0.27 mm	0.42 mm	0.49 mm

On the basis of the assumptions defined in Figure 4, the above data are exact results for areas outside of discontinuity zones, such as the liquid level and the bottom edge disturbance. The results are suitable also for the necessary check and verification of programs for a more complex computational analysis.

3.3 Edge disturbance by restraint of deformation

Following the cylindrical wall is considered at the transition to the bottom slab. Thereby a constant wall thickness is assumed in order to demonstrate clearer the principal influences. Because of the same reason a corner protection is not included in this analysis. However in the practical design, for tanks of the

considered dimensions, an increasing wall thickness at bottom slab (haunch) cannot be dispensed with.

Reasons and consequences of the edge disturbance at the lower ending of a cylindrical shell can be understood easier, if in a first step the deformations are treated without a connection of shell with bottom slab. Figure 7 shows some typical deformation patterns resulting from the thermal curvature without and with restraint. If the wall could be deformed without restraint, due to $\Delta\epsilon_{TL} = 1.8\text{‰}$ an arch shaped bending of 325mm would occur in vertical direction. In reality this deformation is prevented by the restraining stresses as shown in general in Figure 3d and in detail in Figure 6. A residual compressive stress of $n/h = -2\text{MPa}$ is related to a compressive strain $\epsilon_c = -0.53\text{‰}$, which represents also the shortening of the neutral axis $\epsilon_{TL}^{\text{II}}$ in hoop direction. The radius of 40m is thereby shortened by 21mm. The shape of the continuous transition to the bottom slab causes vertical moments and hoop forces, which are designated as edge disturbance.

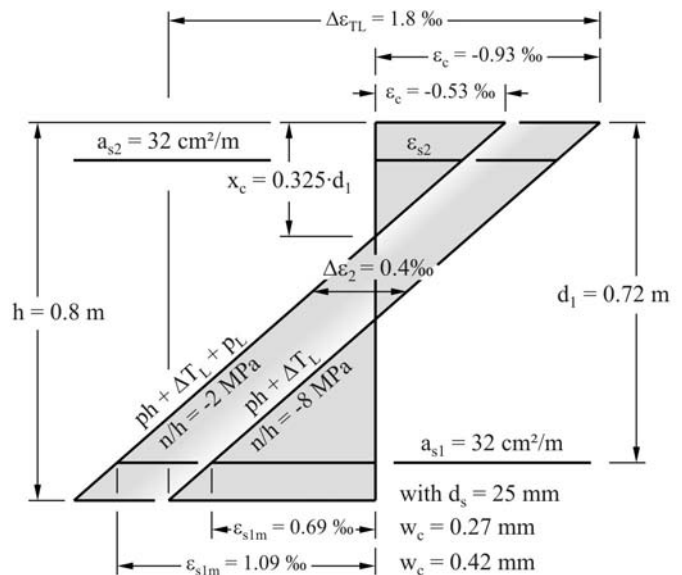


Figure 6: Typical states of strain for restraint curvature

The curve of Figure 8b is based on theory of thin shells of a not cracked concrete section. The curve is also valid for cracked sections, if the ratio from extension stiffness to flexural stiffness ($D^I/B^I = D^{\text{II}}/B^{\text{II}}$) does not change. Figure 5 confirms an approximately constant ratio. Therefore the sectional forces of Figure 8c and 8d are derived by multiplying elongation and curvature acc Figure 8b with the stiffness D^{II} respectively B^{II} .

A typical ratio D^{II}/D^I can be derived easily by means of Figure 6. A reduction of the resulting compressive stress from -8MPa to -2MPa respectively an increase of the hoop tension force from 6.4MN/m to 1.6MN/m causes an increase of strain $\Delta\epsilon_L = 0.4\text{‰}$. This corresponds to a cracked extension stiffness of $D^{\text{II}} = 4.8/0.4\text{‰} = 12,000\text{ MN/m}$. In a not cracked state, the stiffness is calculated with $D^I = E_c \cdot h = 34,500 \cdot 0.8 = 27,600\text{ MN/m}$. Therefore the ratio

$D^{\text{II}}/D^{\text{I}}$ is resulting to $12,000/27,600 = 0.44$. This is in good correlation with the graph in Figure 5.

A hoop tension force n_h greater than 1.6 MN/m respectively $n/h \geq 2 \text{ MPa}$ is occurring up to a height of 4m above the bottom slab as shown in Figure 8c, and vertical through-cracks would occur with this design. This is one of the reasons for the necessity of a thermal corner protection.

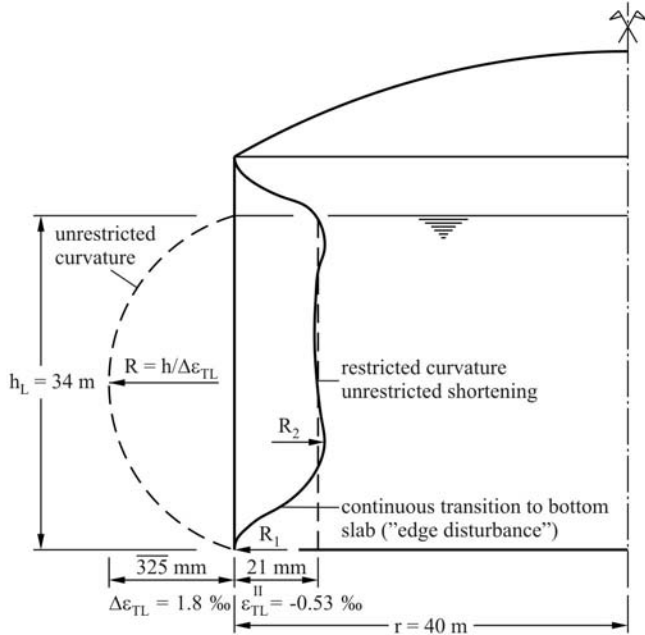


Figure 7: Displacement in radial direction

The curvature $1/R_2$ shown in Figure 8b generates in meridian direction tensile stresses in vertical direction at the inner face (Fig. 8d). They superpose with the gradient $\Delta\epsilon_{\text{TL}}$ in the same direction (Fig. 8e). In contrast to that, the maximum curvature $1/R_1$ at the wall junction acts in contrary direction.

Figure 9 and table 2 show strains and other relevant design data for the action of $\Delta\epsilon_{\text{TL}}$ only (case A and B) and for the superposition of $\Delta\epsilon_{\text{TL}}$ with $1/R_2$

(case C and D). The resulting vertical stress n_v/h is assumed to -2MPa (case A and C) and 0MPa (case B and D). The non prestressed reinforcement is assumed to $d_s = 25\text{mm}/150\text{mm}$. Dead load of wall and roof cause a compression stress of $n_v/h \approx -1\text{MPa}$. The size of the required vertical prestressing depends on the internal gas overpressure. The variation of n_v/h between 0 and -2MPa covers the range to be expected in practice.

By increasing the residual compressive stress n_v/h from 0 to -2MPa , the steel stress is reduced from 395MPa to 344MPa and the crack width from about 0.6mm to about 0.5mm at the location of R_2 acc. Figure 8. In the area above the edge disturbance, a reduction from 324 to 276MPa and from about 0.5mm to about 0.4mm can be achieved.

Crack widths of up to 0.5mm seem acceptable in the special situation of LNG-spill. Because of its short duration they cause no problem with regard to corrosion of reinforcement.

The main aspect is the reparability and structural integrity of the outer containment after such a hazard. This is not endangered by short duration cracks of up to 0.5mm . As for the high stresses in the reinforcement at the inner face, the only reasonable way consists in ensuring a sufficient ductility under the given cryogenic conditions rather than increasing prestressing or reinforcement. The reinforcement bars must sustain the imposed strain of 1.3 to 1.9‰ without risk of rupture. With regard to a safety concept, the ductility should be guaranteed for even higher strains. The conventional notch impact tests (e.g. on charpy specimens) seem not sufficient for the verification of the required ductility considering the real type of notch stresses at the ribs caused by the high bond stresses at cracks.

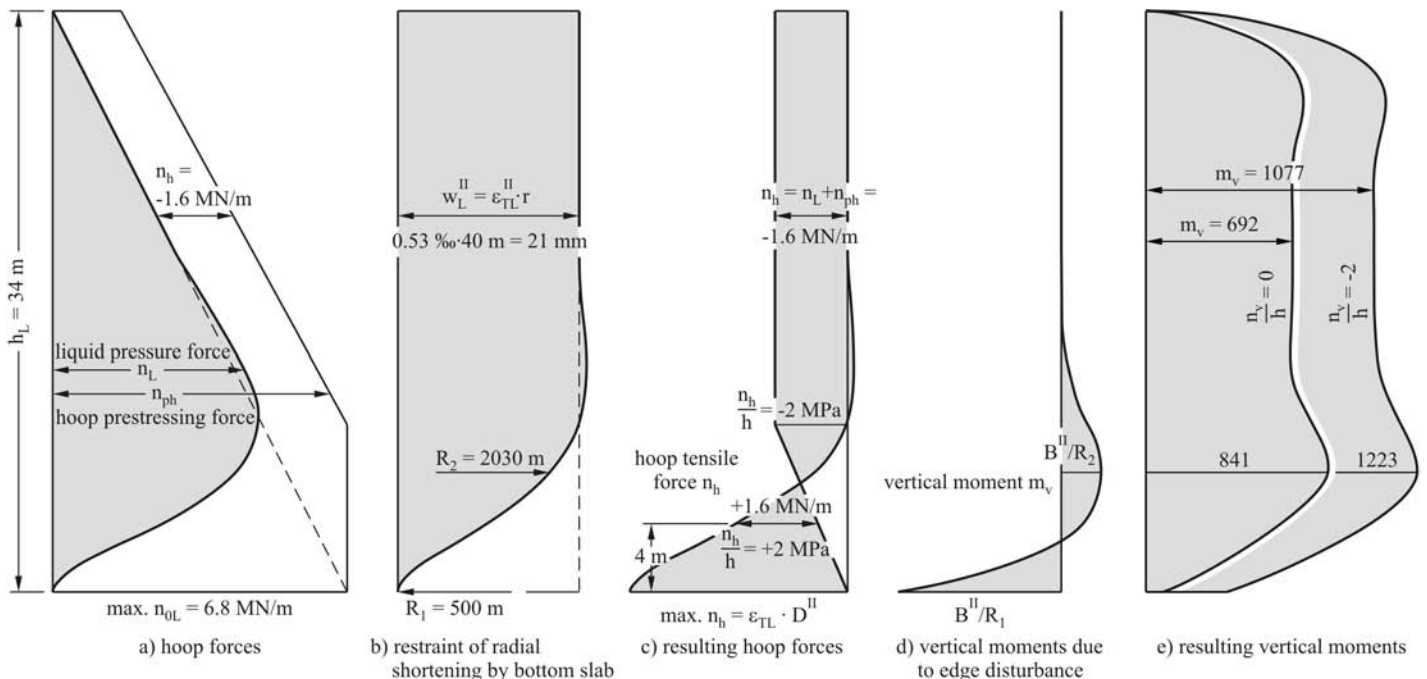


Figure 8: Edge disturbance for typical dimensions (continuous wall thickness 0.80m , no haunch, no Thermal Corner Protection)

Table 2: Values with additional edge disturbances

$\Delta\varepsilon_{TL} + h / R$	line	n_v/h	ε_{s1}	σ_{s1}	w_c [2]	w_c [3]	m_v
‰		MPa	‰	MPa	mm	mm	kNm/m
1.80 + 0	A	-2	1.31	276	0.39	0.42	1077
	B	0	1.54	324	0.49	0.49	692
1.80 + $\frac{0.80}{2030} = 2.19$	C	-2	1.64	344	0.53	0.52	1223
	D	0	1.88	395	0.65	0.60	841

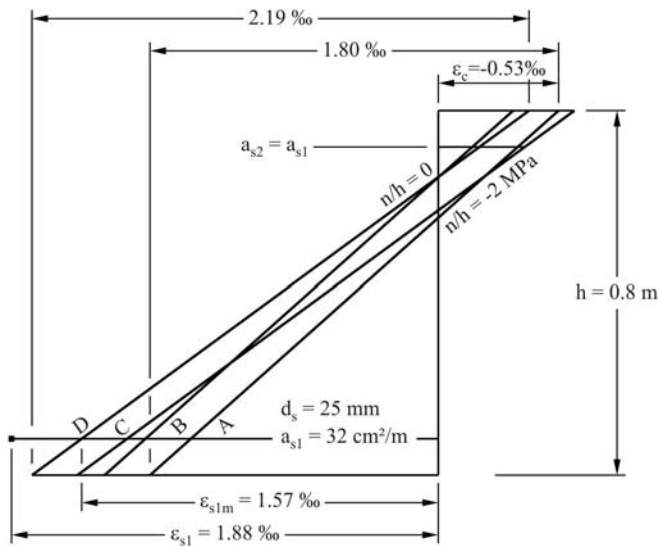


Figure 9: Relevant strains and stresses in vertical direction

4 PRACTICAL DESIGN OF OUTER CONCRETE CONTAINMENTS

Edge disturbance and discontinuity zones with regard to haunches, thermal corner protection, variable liquid levels and other influences can be handled only by computational analysis with suitable programs. Thereby all the questions and assumptions discussed in the previous sections have to be dealt with. First of all it has to be verified, that the applied program is able to model realistically the liquid loads and the imposed thermal deformations, strains, stresses and forces in the cracked structure. This requires thorough tests of the algorithms, which have to depict correctly the basic behavior outlined in the above examples. It would be a fundamental error to expect that even high level standard programs generate correct results automatically only by increasing the “accuracy” of the element net and the iteration process.

Figure 10 shows the results of an analysis (Roetzer et al. 2006) on the simplified system without haunch and thermal corner protection. The moments given for the highest liquid level have to be compared with the superimposed moments of Figure 8d. The correspondence is satisfying.

Only if this first step of verification has been completed successfully further analyses of more complicated systems with edge disturbances at bot-

tom slab and roof ring beam and other discontinuities make sense.

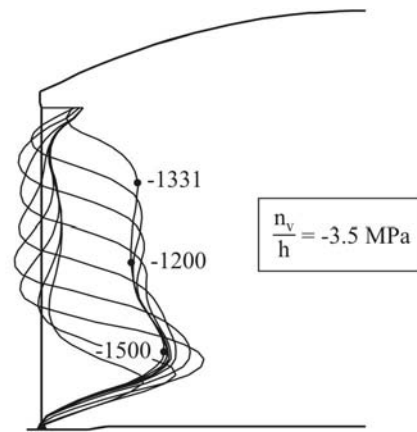


Figure 10: Course of bending moment for different LNG levels

5 CONCLUSION

The outer concrete tank operates as collecting basin, which is exposed to LNG-pressure and thermal shock only in hazard scenarios. Detailed considerations of the problems connected with such a catastrophic event are not always taken seriously, maybe because of the low occurrence probability and because of the opinion that the real course of damage is neither predictable nor afterwards reconstructable.

The corresponding codes and standards do not really refute this interpretation. They provide a lot of formal regulations, but give no precise indications to the basic requirements. Such an approach is not justifiable, neither economically nor in the face of the demanded protection of health and safety.

The effort for a consistent analysis and design of the components and assemblies and for the development and procurement of appropriate materials with regard to a safe and reliable behaviour also in hazard situations is minor in comparison to possible damages.

6 REFERENCES:

- BS 7777. 1993. Flat Bottomed, Vertical, Cylindrical Storage Tanks for Low Temperature Service. Part 3: Recommendations for the Design and Construction of Prestressed and Reinforced Concrete Tanks. London: BS
- DIN 1045-1. 2001. Concrete, reinforced and prestressed concrete structures – Part 1; Design and construction. Berlin: Beuth
- Noakowski, P. & Schäfer, H.G. 2003: Steifigkeitsorientierte Statik im Stahlbetonbau. Berlin: Ernst & Sohn
- Roetzer, J., Douglas, H. & Maurer, H. 2005 & 2006. Hazard and Safety Investigations for LNG-Tanks. Part 1: Earthquakes. Part 2: Explosions. Part 3: Liquid Spill. LNG-Journal